8C.1 A STUDY ON TROPICAL CYCLONE STRUCTURE CHANGES AND ORGANIZED CONVECTIONS ASSOCIATED WITH TC-ENVIRONMENT INTERACTIONS

Buo-Fu CHEN*, Cheng-Shang LEE
Department of Atmospheric Sciences, National Taiwan University, Taipei, Taiwan

1. INTRODUCTION

Scientists' ability to forecast tropical cyclone (TC) tracks has improved dramatically in the past few decades. To improve our understanding of TCs' impacts further, many studies have focused on the intensity and structure changes of TCs. In the western North Pacific, structure forecasting is more important than intensity forecasting because the structure of TCs is closely related to the tremendous rainfall associated with TCs, which causes much damage and is important to the development of quantitative precipitation forecasting techniques.

Some studies (e.g. Chien et al. 2008; Chien and Kuo, 2011; Lee et al., 2011) have shown that southwesterly flows were an important ingredient leading to the asymmetric convections associated with typhoons, such as Typhoon Morakot (2009) and Mindulle (2004), which caused lots of damages in southern Taiwan. We noted that, in those monsoon-influenced typhoons, at least two different modes of active and long-lasting convective systems occurred when TCs encountered strong southwesterly flows. The first mode was the mesoscale convective systems that developed from distant rainbands, which were usually concentric to the inner-core. We will use the term "outer-MCSs" (OMCSs) to represent this kind of convective systems. On the other hand, the second mode was principle-rainbands (Willoughby et al. 1984) that became very active. We will use the term "Enhanced rainbands" (ERBs) to call them.

The structure of TCs may evolve according to internal and external processes. The external processes are related to the environments in which TCs are embedded, such as vertical wind shears, moisture patterns and large scale circulations. Both OMCSs and ERBs usually caused a thick and vast region of stratiform precipitation to develop. Furthermore, they are greater in scale than rainbands in a typical hurricane. The convective effects of these two types of active and long-lasting convective systems may be considered as noticeable external forcing to TC structures.

*Corresponding author address: Buo-Fu Chen, Department of Atmospheric Sciences, National Taiwan University, e-mail: bfchen@nat.as.ntu.edu.tw

In this study, we will try to identify the OMCSs and ERBs that may associate with the TC-environment interactions, firstly. Then, we will try to figure out whatever the characteristics of TC's structure changes are related to OMCSs and ERBs.

2. METHODOLOGY

A two-stage procedure, which included using hourly infrared channel-1 cloud-top temperature dataset (IR1) and passive micro-wave images (PMW), was applied to investigate long-lived and active convective systems embedded in TCs in the western North Pacific from 1999 to 2009. The IR1 dataset was obtained from a digital archive at Kochi University in Japan. It was on a 5-km grid with a spatial coverage of 20°S–70°N, 70°–160°E. The PMW images were obtained from the Naval Research Laboratory tropical cyclone web page.

IR1 images were used to identify the convective features that had a considerable large cold cloud shield, sustained for a considerable long duration and occurred in the region extending from the TC's center with a radius of 1000 km. (Fig 1(a) and 1(c)) These systems were defined initially when any contiguous cold cloud shield (CCS) that exhibited IR1 brightness temperatures (T_B) colder than -75ºC first exceeded 36000 km^2 in size. Then, two types of CCSs in the next frame (one hour later) were used to track the active and long-lasting convections. When either a CCS that had T_B colder than -75ºC and extended larger than 36000 km^2 in size (CCS_{-75}) or a CCS that had T_B colder than -65ºC and extended larger than 72000 km^2 in size (CCS_{-65}) overlapped the previous CCS_{-75} with an area larger than 50%, the convective system was regarded as "active". Furthermore, if it remained active for a period greater than 6 hours, it was chosen to inclusion in the second stage of the selection procedure. In the first stage, 603 active and long-lasting convections were selected.

The objective of the second stage of the selection procedure was to distinguish two kinds of convective systems: outer-MCS (OMCS) and enhanced-rainband (ERB). If an convective system met the criteria as follows, it was regarded as an OMCS (Fig. 1(b)). First, an OMCS is associated with convections that develop from distant rainbands. Thus,

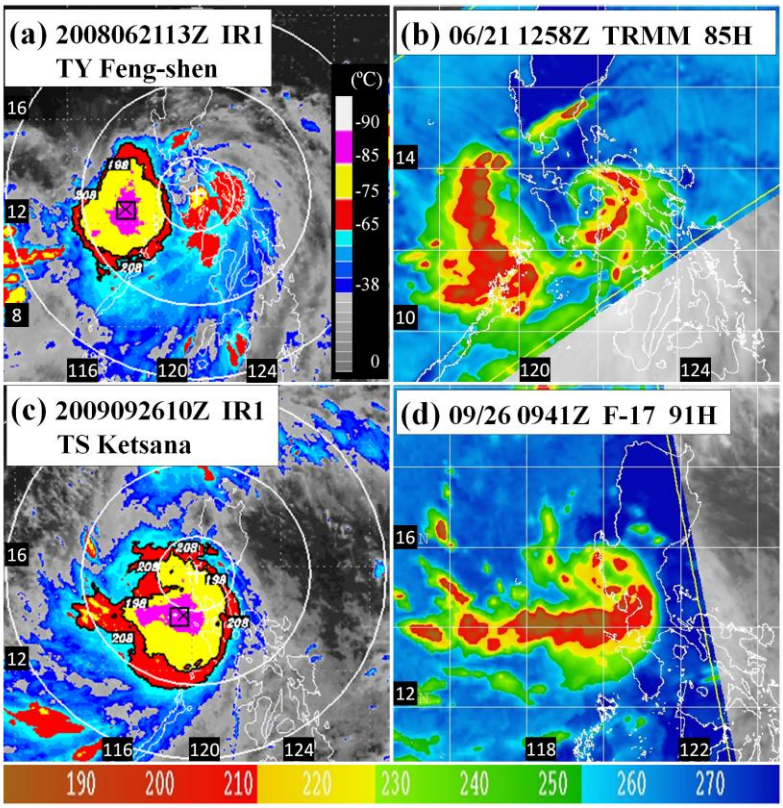

Fig 1. IR1 images and PMW images－(a) and (b), the OMCS of Fung-shen (2008); (c) and (d), the ERB of TS Ketsana (2009).

a convective line should exist in the PMW image and is concentric to the inner-core of the TC. Second, the mean distance from an OMCS's center to the TC's center of the OMCS's lifetime must be not less than 200 km. On the other hand, if an convective system met the criteria as follows, it was regarded as an ERB (Fig. 1(d)), which occurred when a spiral rainband became extremely active. First, the convective line spiraling into the inner-core should exist in the PMW image. Second, the CCS_{-65} in the IR1 images should be similar in size to or greater in size than the inner-core cold cloud shield. Third, the mean distance from an ERB's center to the TC's center of the ERB's lifetime must be not less than 100 km.

To sum up, after operating two stage of case selecting procedures, 90 inner-MCSs and the 109 outer-MCSs were selected from 1999 to 2009.

3. CLIMATOLOGY OF OMCSS AND ERBS

Approximately 34% (111/322) of all TCs produced at least one ERB or OMCS during their lifetimes. Furthermore, 21% and 22% of all TCs produced at least one ERB or OMCS, respectively. The mean durations of OMCSs and ERBs were 10.3 hr and 12.2 hr, respectively. Figure 2(a) shows the tracks of OMCSs and the probability density functions (PDF) of OMCSs calculated using hourly OMCS track records in a 2° × 2° latitude–longitude box. According to Figure 2(a), the OMCSs were widely distributed in the western North Pacific. On the other hand, as shown in Figure 2(b), the ERBs, similar to the OMCSs, were also widely distributed in the western North Pacific.

We also examined the synoptic environments of OMCSs/ERBs when they occurred south of TC's centers and north of TC's centers. The composite environments were conducted based on NCEP-GFS grid data and exhibited significant difference to each other. The south-type ERBs/OMCSs developed in environments influenced by south-westerly flows. These environments were similar to the environment described in Chien et al. (2008). On the other hand, the north-type ERBs/OMCSs developed in environments influenced by the north-easterly flows, which were similar to the environment described in Wu et al. (2009). In this study, we only focus on the 85 south-type OMCSs and 80 south-type ERBs, which may associated with the interactions of TCs and south-westerly flows.

Figure 3 shows the distribution of “mean distance” of south-type ERBs and south-type OMCSs. The “mean distance” was defined as the average of the distances between the center of one ERB/OMCS and the center of the TC that produced this ERB/OMCS at every hour in this ERB’s/OMCS’s lifetime. The distribution of the mean distances for ERBs ranged from 100km to 350km and had an average of 183km. On the other hand, the distribution of the mean distances for OMCSs ranged from 200km to 650km and did not have an obvious peak.

4. INFLUENCE ON TC INTENSITY AND SIZE

In this section, the characteristics of structural changes, which conducted based on JTWC best track data, associated with OMCSs and ERBs were presented. Fig.4 showed the composite time series of the normalized intensity and normalized size for the OMCSs, the ERBs and the cases of TCs that encountered strong / weak south-westerly flows.

The group OMCSs and the group ERBs included the OMCS/ERB cases that occurred from June to September during 2002~2009. And, the samples of these two groups should have intensities greater than 35kt, and be 200km away from the land during the period between 24 hours before the initial time of OMCSs/ERBs and 24 hours after the terminal time of OMCSs/ERBs. Therefore, the group OMCSs and the group ERBs had 16 and 13 samples, respectively. Furthermore, the compositing normalized intensity and normalized size of TCs were done relative to the initial time of OMCSs and ERBs for the OMCSs and ERBs, respectively.

The samples of the group strong SW-flows and the group weak SW-flows were 60-hourly-long periods selected from the lifetime of those TCs that did not produced any OMCSs or ERBs. All samples should occur from June to September during 2002~2009 and meet the criteria as follows: a) the TC was south to 26°N and west to 145°E, b) the TC was 200km away from the land during the period between 24 hours before and 36 hours after the reference time, c) these groups should have the same intensity distribution to the 13 ERBs and 16 OMCSs.

The group strong SW-flows (weak SW-flows) include 29 samples of period that met the criteria above and had the 29 strongest (weakest) south-westerly flows at the reference time. The strength of south-westerly flows is defined as the average wind speed at 850mb in a box, which is 4° south to 12°south and 12° west to 8° east with respect to the TCs’ center. These two groups could represent the characteristics of structural change when a TC encountered strong and weak south westerly flows, but did not produce active and long-lasting convections, respectively. As shown in Fig 4 (a) and 4(b), when ERBs occurred, the TCs usually increased its size with a faster rate and the intensification rate remained the same. However, when an outer MCS occurred, the increasing rate of size remained the same but the intensification rate became slower.

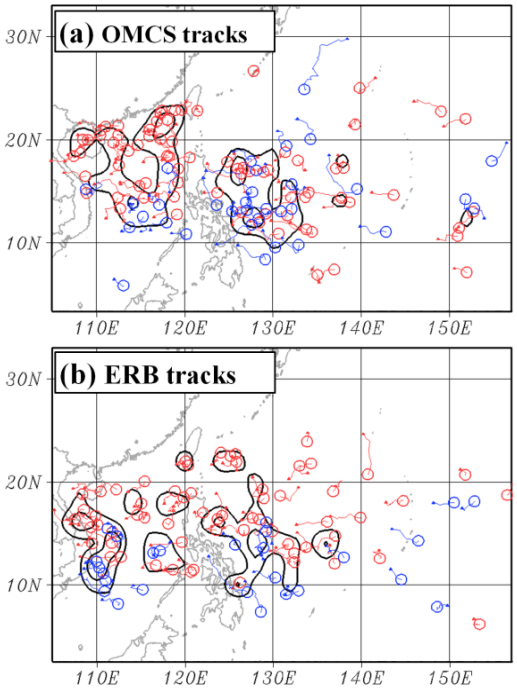

Fig 2. (a) The tracks of OMCSs and PDF of OMCSs (contour in the interval of 0.1 12hr/yr). (b) Same as in (a), but for ERBs. Red tracks (blue tracks) represent the OMCS/ERB that occurred during June - September (October - May).

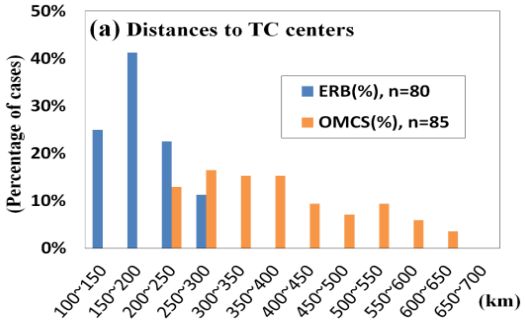

Fig 3. Histogram showing the distribution of the distances between 80 south-ERBs’ centers to the TCs’ centers, and the distribution of the distances between 80 south-OMCSs’ centers to the TCs’ centers.

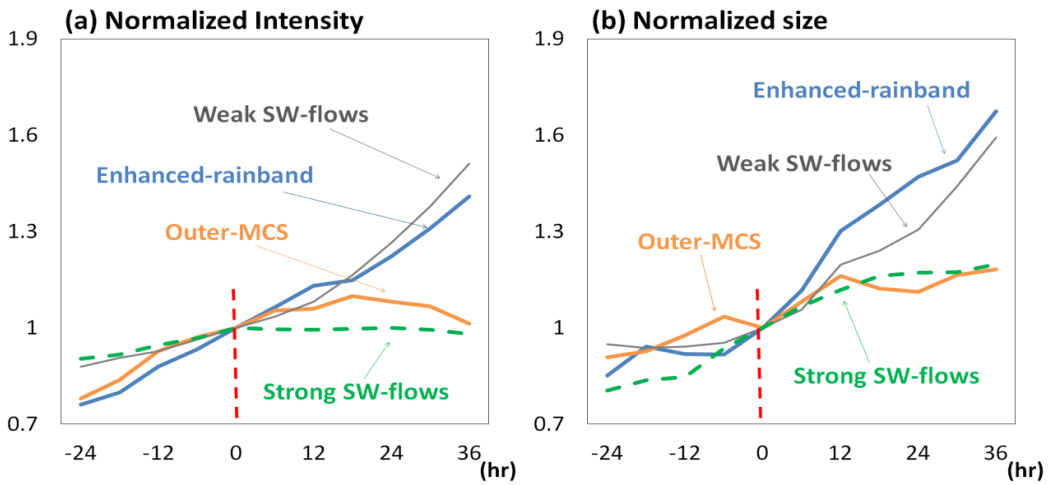

Fig 4. Composite time series of the normalized intensity (a) and normalized size (b) for the OMCS, the ERBs and cases of TCs that encountered strong / weak south-westerly flows (strong SW-flows / Weak SW-flows).

5. SUMMARY

In the western North Pacific, active and long-lasting convective system, such as OMCSs and ERBs, occurred while TCs interacted with strong environmental flows. Furthermore, it is noteworthy that ERBs and OMCSs affected TCs' structures differently.

It is suggested that, when an ERB occurred, the cyclonic PV was generated in the midtroposphere stratiform precipitation region. Then, the cyclonic PV, which could be an important PV source to the core (May and Holland1999), was wrapping into the inner-core. As a result, the TC usually increased its size with a faster rate. On the other hand, although low θ_e air was brought into the inflow boundary layer by the downdrafts of the ERB and may reduce eyewall convections, this negative effect on TC intensification (Barnes et al.1983; Powell 1990) may be compensated by the inward-transported PV in the midtroposphere. Thus, the intensification rate remained the same. However, when an OMCS occurred, the cyclonic PV generated in the midtroposphere stratiform precipitation region was too far away from the TC's center to be wrapped into the inner-core. Low θ_e air, brought into the inflow boundary layer by the downdrafts, may reduce eyewall convections. Therefore, the intensification rate of TCs became slower when an OMCS occurred.

The ongoing work, which will be conducted by model simulated data, will focus on why OMCSs and ERBs affected TC structure differently, and on environmental factors and mesoscale mechanisms that determine whether an OMCS or an ERB will develop.

6. REFERENCES

Barnes, G. M., E. J. Zipser, D. Jorgensen, and F. Marks Jr., 1983: Mesoscale and convective structure of a hurricane rainband. *J. Atmos. Sci.*, **40,** 2125–2137.

Chien, F. C., and H. C. Kuo, 2011: On the extreme rainfall of Typhoon Morakot (2009). *J Geophys Res-Atmos*, **116**, D05104.

Chien, F. C., Y. C. Liu, and C. S. Lee, 2008: Heavy rainfall and southwesterly flow after the leaving of Typhoon Mindulle (2004) from Taiwan. *J Meteorol Soc Jpn*, **86(1)**, 17-41.

C. S. Lee, Elsberry, R. L., C. C. Wu, and T. C. C. Wang, 2011: Advances in understanding the "Perfect Monsoon-influenced Typhoon": Summary from International Conference on Typhoon Morakot (2009). *Asia-Pac J Atmos Sci*, **47(3)**, 213-222.

May, P. T., and G. J. Holland, 1999: The role of potential vorticity generation in tropical cyclone rainbands. *J. Atmos. Sci.*, **56,** 1224–1228.

Powell, M. D., 1990: Boundary layer structure and dynamics in outer hurricane rainbands. Part II: Downdraft modification and mixed layer recovery. *Mon. Wea. Rev.*, **118,** 918–938.

Wu, C.-C., K. K. W. Cheung and Y.-Y. Lo, 2009: Numerical study of the rainfall event due to interaction of Typhoon Babs (1998) and the northeasterly Monsoon. *Mon. Wea. Rev.*, **137**, 2049-2064.

Willoughby, H. E., F. D.Marks, and R. J. Feiberg, 1984: Stationary and moving convective bands in hurricanes. *J. Atmos. Sci*., **41**, 3189–3211.